



Analogue-based design, synthesis and molecular docking analysis of 2,3-diaryl quinazolinones as non-ulcerogenic anti-inflammatory agents [☆]

E. Manivannan ^{*}, S. C. Chaturvedi

School of Pharmacy, Devi Ahilya Vishwavidyalaya, Ring Road, Indore 452017, MP, India

ARTICLE INFO

Article history:

Received 18 April 2011

Revised 4 June 2011

Accepted 8 June 2011

Available online 15 June 2011

Keywords:

Analogue-based design

2,3-Diaryl quinazolinones

COX-1

COX-2

Anti-inflammatory activity

Ulcerogenic activity

Molecular docking

ABSTRACT

In our effort to identify potent gastric sparing anti-inflammatory agents, a series of methyl sulfonyl/methyl sulfonyl substituted 2,3-diaryl quinazolinones were designed by analogue-based design strategy and synthesized for biological evaluation. Subsequently, the compounds were evaluated for both cyclooxygenase inhibitions by ovine COX assay and carrageenan-induced rat paw edema assay. All the methyl sulfonyl substituted quinazolinones were exhibited promising anti-inflammatory activity. In particular, 6-bromo-3-(4-methanesulfonyl-phenyl)-2-phenyl-3H-quinazolin-4-one (**18**), 7-chloro-3-(4-methanesulfonyl-phenyl)-2-phenyl-3H-quinazolin-4-one (**19**), 3-(4-methanesulfonyl-phenyl)-2-(4-methoxy-phenyl)-3H-quinazolin-4-one (**21**) and 6-bromo-3-(4-methanesulfonyl-phenyl)-2-(4-methoxy-phenyl)-3H-quinazolin-4-one (**22**) emerged as the most active compounds in the series. The results of ulcerogenic activity assay suggest that these compounds are gastric safe compared to indomethacin. The molecular docking analysis was performed to understand the binding interactions of these compounds to COX-2 enzyme. The results from the present investigation suggests that 2,3-diaryl quinazolinones as a promising template for the design of new gastric safe anti-inflammatory agents, which can be further explored for potential anti-inflammatory activity.

© 2011 Elsevier Ltd. All rights reserved.

1. Introduction

Non-steroidal anti-inflammatory drugs (NSAIDs) are among the most widely prescribed medicines for the treatment of pain, fever, inflammation and arthritis.¹ The classical NSAIDs produce their therapeutic benefit by inhibiting cyclooxygenase enzymes and thus reducing the formation of inflammatory mediator prostaglandins.² The discovery of existence of two distinct isoforms of COX demonstrated that the side effects of NSAIDs such as gastric irritation, ulcer and gastric perforation are mainly due to inhibition of physiological enzyme COX-1 along with the desired blockade of COX-2 enzyme.^{3–6} The structure of COX-1 and COX-2 enzymes and their inhibitors have been thoroughly investigated for more than two decades of research. This led to the development of many of selective COX-2 inhibitors, which are almost free of gastric side effects. Recent studies on this field show that COX-2 inhibitors are attractive molecular target for the development cancer chemotherapy^{7–9} and neurological diseases such as Parkinson¹⁰ and Alzheimer's diseases.¹¹

Selective COX-2 inhibitors belonging to different structural classes such as vicinal diaryl heterocycles, diaryl carbocycles and

heteroaryl-ethers have been developed as pharmacophore for anti-inflammatory activity.¹² Soon after the discovery of some selective COX-2 inhibitors namely, celecoxib, rofecoxib, valdecoxib and parecoxib as gastric safe anti-inflammatory drugs, researchers focused extensively on tricyclic template based COX-2 inhibitors.^{13–16} Variations of the central ring in tricyclic COX-2 inhibitors have already generated a number of potent derivatives with thiazole, triazole, imidazole, isoxazoline, pyridine, pyranone, pyridazone, pyrimidine, pyran, indole, benzothiazole, benzotriazole, benzimidazole, and benzopyran central ring scaffold.^{17–30} In the present investigation, we were focused on designing novel COX-2 inhibitors based on quinazolinone template as influenced by the facts such as limited citations as bicyclic central scaffolds as COX-2 inhibitors and recognition of quinazolinone heterocycle in a number of natural anti-inflammatory alkaloids like rutaecarpine^{31–33} and tryptanthrin.^{34–36}

2. Results and discussion

2.1. Analogue-based design

A series of anti-inflammatory compounds possessing 2,3-diaryl quinazolinones were designed based on 'analogue-based' design strategy with the application of quantitative structure–activity relationship analysis. The selection of diaryl quinazolinone pharmacophore was motivated by its good compliance with both

[☆] A part of the work was presented in European Drug Discovery conference Miptech-2009, Basel, Switzerland.

^{*} Corresponding author. Tel.: +91 731 2100605, mobile: +91 8982677476.

E-mail address: drmanislab@gmail.com (E. Manivannan).

geometrical and surface properties necessary for COX-2 inhibition. In search of structural similarity, the design foresaw replacement of the 'central scaffold' **A** with a bicyclic structure quinazolinone, and followed by introduction of reasonable diversity in the rest of the structures **B**, **C**, **D** and **E** according to Figure 1. The specific structural features were selected for designing the new anti-inflammatory compounds with reasonable justification. The choice of quinazolinone heterocycle as a central core was fundamental due to its presence in the potent anti-inflammatory natural alkaloid rutaecarpine, and tryptanthrin. The introduction of 'diaryl' structural motif was due to its recognition as pharmacophore¹⁰ for cyclooxygenase inhibition and as most of the tricyclic COX-2 selective inhibitors celecoxib, rofecoxib, valdecoxib and parecoxib constituted by this chemical feature. Additional $-\text{SO}_2\text{CH}_3$ group was based on fact that either a *para*- SO_2CH_3 or a *para*- SO_2NH_2 substituent on one of the phenyl rings is necessary for selectivity that the group inserts into a secondary side pocket present in the COX-2 enzyme active site.¹² Electron withdrawing group on central core was introduced since the addition of small lipophilic electron withdrawing groups found to increase the COX inhibitory activity as it interacts with the aromatic amino acid residues of COX isozymes. Substituents on phenyl ring were decided on the basis of quantita-

tive structure–activity relationship of various bicyclic analogs with good COX-2 inhibitory potency.^{19–23}

2.2. Shape based searching of the designed molecules

Shape complementarity between the protein and ligand plays a crucial role in the binding of ligand to receptor. Since the basic skeleton or scaffold of the molecule influences overall steric shape of the molecule it is important to evaluate whether the template selected permits proper orientation of the diaryl groups to enable the binding of the ligand to enzymes active site. With this understanding, the designed molecules were probed for shape similarity using shape query SC558, a structurally analogous potent COX-2 inhibitor extracted from pdb file 1cx2 employing PHASE module of molecular modeling software Schrödinger. The shape similarity of the designed molecules to SC558 is given by similarity index which can have values from 0 to 1. All the designed molecules exhibited similarity index values greater than 0.5 which suggest that molecules are capable of achieving good binding affinity to COX-2 enzyme. The molecular alignment of the designed analogs to the shape query SC558 is shown in Figure 2.

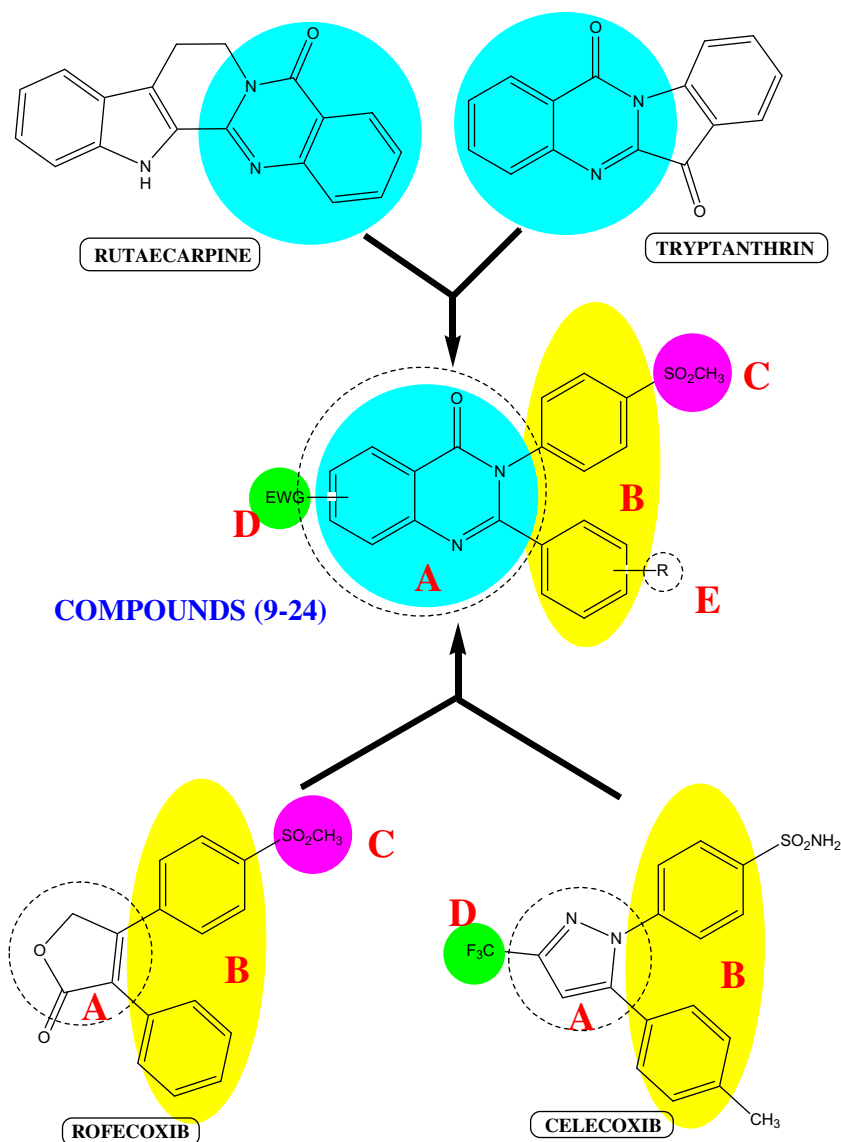


Figure 1. Analogue-based design of anti-inflammatory quinazolinones.



Figure 2. The molecular alignment of the designed analogs to the shape query SC558.

2.3. Chemistry

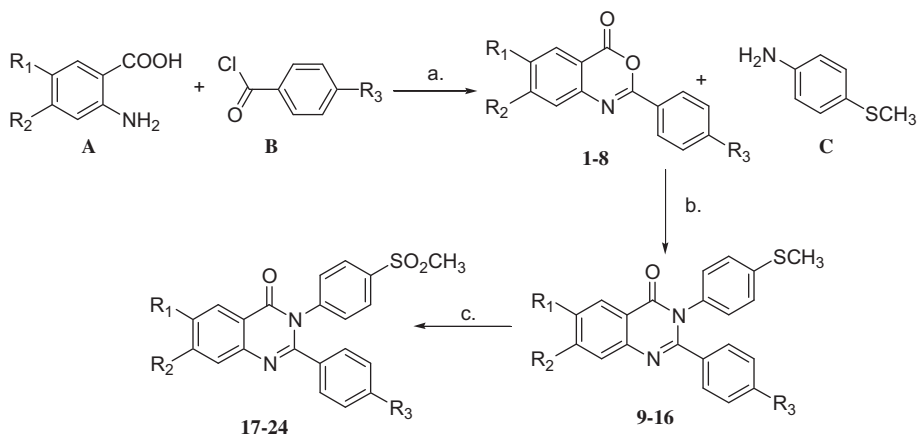
A set of 2,3-diaryl-3*H*-quinazolin-4-ones that possess a SCH₃ or SO₂CH₃ substituent at the para position of one of the aryl rings with or without a methoxy substituent on the other aryl ring, along with H, F, Cl and Br substituents on central quinazolin-4-one ring were designed and synthesized for COX-2 inhibitory potential. The synthetic strategy adopted for the synthesis of title compounds has been depicted in Scheme 1. Sixteen analogues of 2,3-diaryl-3*H*-quinazolin-4-ones **9–24** were synthesized. The starting materials, substituted 2-phenyl-3*H*-benzoxazin-4-ones **1–8**, were synthesized using the known procedure.³⁷ Various anthranilic acids (unsubstituted, 4-chloro, 4-fluoro and 5-bromo derivatives) were reacted with acid chlorides in pyridine at 25 °C, corresponding 2-phenyl-benzoxazin-4-ones were obtained as crystalline products. The subsequent reflux with 4-methylthio aniline in glacial acetic acid gave para –SCH₃ substituted 2,3-diaryl-3*H*-quinazolin-4-ones **9–16**. Further oxidation of these compounds with ‘oxone’ in tetrahydrofuran and methanol mixture yielded 4-methyl sulfonyl substituted 2,3-diaryl-quinazolin-4-ones **17–24**. The synthesis of benzoxazin-4-ones involves acylation of both the amine and acid functions of the appropriate anthranilic acid by the acid chloride followed by ring closure of the intermediate affected via an intramolecular nucleophilic displacement of the corresponding

benzoic acid. This method has the advantage of being a one-pot synthesis and gave significantly good yields.

The physicochemical properties were calculated by standard methods and the structures of the synthesized compounds were confirmed by IR, NMR, Mass and elemental analysis. The IR spectrum of the substituted quinazolin-4-one compounds (**9–24**) showed characteristics prominent peaks in at 1680–1710 cm^{−1} (C=O of 4-keto-quinazolinone), which further confirms the formation of the title compounds. The compounds were also showed disappearance of bands at 1600–1650 cm^{−1} (N–H deformation) and 3460–3500 cm^{−1} (N–H stretching) due to conversion of free amino group into cyclic nitrogen. Halogen containing quinazolin-4-ones showed the characteristic absorption bands at 590–760 cm^{−1} (C–X stretching). The conversion of methylsulfanyl (–SCH₃) to methylsulphonyl (–SO₂CH₃) was detected by the δ shift from 2.47 to 3.34 ppm for CH₃ protons in the NMR spectrum. The –OCH₃ protons appeared in the chemical shift range of 3.6–3.8 ppm. Other aromatic protons appeared as multiplets in δ 7.1 to 8.5 ppm. Further the mass spectrum [FAB-MS] showed a molecular ion peak (M⁺) for benzoxazin-4-ones and quinazolin-4-ones respectively. In the ESI-MS spectra, molecular ion [M⁺] peaks, which appeared at different intensities, confirmed the molecular weights of the synthesized compounds. Molecular ion peaks were the base peaks for most of the compounds. Appearance of an isotope peak [M⁺+2] as intense as the molecular ion peak has confirmed shows the presence of halogen atom in compounds. All the synthesized compounds were also characterized by elemental analysis and its experimental values coincided with the calculated values and errors lay within $\pm 0.3\%$ of the calculated values.

2.4. In vitro cyclooxygenase inhibitory activity

Biological evaluation of title compounds with regard to COX-1 enzyme inhibition, the methyl sulfanyl/methyl sulphonyl substituted 2,3-diaryl-3*H*-quinazolin-4-ones **9**, **13** and **17–24** proved to be slightly active, with percentage inhibition values ranging from 0 to 30% at a concentration of 20 μ M. Among all the screened compounds, the compounds substituted with chlorine and methyl sulphonyl groups on 2,3-diaryl-3*H*-quinazolin-4-ones **19** proved to be practically inactive as they have shown 0% inhibition at 20 μ M concentration. In case of COX-2 enzyme inhibition, all the screened compounds showed modest to better activity with percentage inhibition values ranging from 40% to 100% at a concentration of 20 μ M. The 2,3-diaryl-3*H*-quinazolin-4-ones substituted with bromo and methyl sulphone **18** and chloro methyl sulphonyl **19**



Scheme 1. Reagents and conditions: (a) dry pyridine, 25 °C, 1–2 h; (b) CH₃COOH, reflux, PTSA; (c) oxone, THF, MeOH, 2–3 h.

possess a higher COX-2 inhibitory activity with a percentage of 88–100% maximum. The in vitro COX-1 and COX-2 inhibitory activity results (Table 1) indicate that overall the methyl sulphonyl substitution on all the compounds increase the COX-2 selectivity in varying magnitude depending upon the presence of other aromatic substitution. Comparable COX-2 selectivity with reference compound celecoxib was observed when 2,3-diaryl-3H-quinazolin-4-ones ring substituted with Br, and Cl groups.

2.5. In vivo anti-inflammatory activity

All the compounds were screened for in vivo anti-inflammatory activities at 50 mg/kg body weight dose level with carrageenan-induced rat paw edema using indomethacin as reference drug. The paw edema induced by subplantar injection of carrageenan was more prominent in the group treated with carboxymethyl cellulose sodium (CMC-Na:Vehicle) where indomethacin exerted 58.16% anti-inflammatory effect after 180 min. Among the tested compounds of 2,3-diaryl-3H-quinazolin-4-ones series (Table 2), **15**, **18**, **19**, **21**, and **22** exhibited more than 45% edema inhibition and decreased the difference in paw thickness comparable to that of a group received indomethacin ($p < 0.05$). The anti-inflammatory effect of compound **22** has comparable effect of indomethacin at 10 mg/kg dose. All test compounds of the series, anti-inflammatory activity was retained up to six hours unlike indomethacin, the activity was started decreasing after 4 h. The efficacy of test compounds was comparable to that of indomethacin, but with a longer duration of action. This phenomenon may partly be due to the low systemic bioavailability of test compounds following oral dosing, due to efficient first-pass metabolism and some degree of intestinal metabolism. 2,3-Diaryl-3H-quinazolin-4-ones **15**, **18**, **19**, **21** and **22** were identified as potent anti-inflammatory compounds. Among them, **15** is the only compound with methylsulfonyl ($-\text{SO}_2\text{CH}_3$) at R_4 substitution position and the rest of the compounds have

methyl sulphonyl ($-\text{SO}_2\text{CH}_3$) at R_4 . Halogen atoms or methoxy groups at R_1 and R_3 position of 2,3-diaryl-3H-quinazolin-4-ones appears to have a positive effect on the anti-inflammatory potency of these compounds.

2.6. Ulcerogenic activity

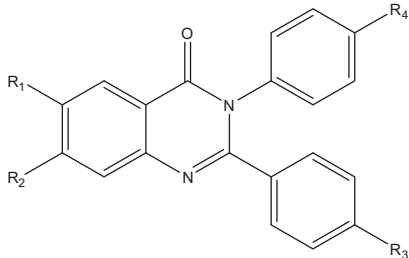
Although the activities of many synthesized compounds were comparable to the reference drugs, the gastric toxicity experiments were only performed with most potent compounds of substituted 2,3-diaryl-3H-quinazolin-4-ones series **18**, **19**. The most active compounds of the series and indomethacin were given orally to rats and they were sacrificed after treatment for determining the ulcerogenic index of the said compounds. None of the compounds showed any ulcerogenic effects (Table 3) in the gastric mucosa at a total dose of 100 mg/kg body weight in fasted rats. From the results of the histopathological studies, it is evident that in all the groups treated with compounds **18**, **19**, the structure of gastric mucosa is quite normal. Capillary dilatation was observed at the most superficial region in few parts of the gastric mucosa. The cross section also showed that the surface epithelium was continuous and normal. Gastric ulcers were observed in all the animals treated with 10 mg of Indomethacin. The superficial regions of the gastric mucosa of these animals showed multiple areas of erosions and hemorrhage. Erosions were not observed beyond the muscularis mucosa. The layers other than the superficial mucosa appeared normal. The gland beneath and around the ulcer areas were dilated and distorted. The glands in this region were also dilated.

2.7. Molecular docking

With the aim of getting insights into the structural basis for its activity, 2,3-diaryl-3H-quinazolin-4-ones (compounds **9**–**24**) were docked into the active site of COX-2 enzyme. The Glide docking

Table 1

In vitro COX-1 and COX-2 enzyme inhibition data for substituted 2,3-diaryl-3H-quinazolin-4-ones



Compound	Substitution				Percentage inhibition ^a			Physical properties	
	R ₁	R ₂	R ₃	R ₄	COX-1 (20 μM)	COX-2 (20 μM)	Selectivity COX-1/COX-2	TPSA	Molecular volume
9	H	H	H	SCH ₃	12	40	0.3	34.897	305.736
10	Br	H	H	SCH ₃	—	—	—	34.897	323.622
11	H	Cl	H	SCH ₃	—	—	—	34.897	319.272
12	H	F	H	SCH ₃	—	—	—	34.897	310.667
13	H	H	OCH ₃	SCH ₃	30	56	0.536	44.131	331.282
14	Br	H	OCH ₃	SCH ₃	—	—	—	44.131	349.167
15	H	Cl	OCH ₃	SCH ₃	—	—	—	44.131	344.818
16	H	F	OCH ₃	SCH ₃	—	—	—	44.131	336.213
17	H	H	H	SO ₂ CH ₃	13	42	0.310	69.039	319.039
18	Br	H	H	SO ₂ CH ₃	4	100	0.04	69.039	336.924
19	H	Cl	H	SO ₂ CH ₃	0	88	—	69.039	332.575
20	H	F	H	SO ₂ CH ₃	15	63	0.238	69.039	323.97
21	H	H	OCH ₃	SO ₂ CH ₃	24	51	0.471	78.273	344.585
22	Br	H	OCH ₃	SO ₂ CH ₃	7	66	0.106	78.273	362.47
23	H	Cl	OCH ₃	SO ₂ CH ₃	12	72	0.167	78.273	358.121
24	H	F	OCH ₃	SO ₂ CH ₃	29	64	0.453	78.273	349.516
Celecoxib	—	—	—	—	3	94	0.032	—	—

^a Values represents means of two determinations acquired using an ovine COX-1/COX-2 assay kits, nd - COX-1/COX-2 Inhibitory activity not determined.

Table 2

In vivo anti-inflammatory activity data and docking results for substituted 2, 3-diaryl-3H-quinazolin-4-ones

Compound	Percentage edema inhibition				Docking score GLIDE XP SCORE
	90 min	180 min	270 min	360 min	
9	29 ± 1.73*	32 ± 0.69***	34 ± 0.48*	38 ± 1.33*	−7.4254
10	30 ± 0.27**	33 ± 1.82*	35 ± 1.36*	39 ± 0.24*	−3.38017
11	31 ± 1.26*	32 ± 0.69*	34 ± 0.48*	39 ± 1.54*	—
12	29 ± 1.46**	36 ± 1.04*	39 ± 1.44**	40 ± 1.25*	−7.70532
13	30 ± 0.47*	34 ± 1.34*	38 ± 1.77**	40 ± 1.89*	−7.11189
14	32 ± 1.45*	35 ± 0.14*	39 ± 1.46	42 ± 1.81*	−3.40755
15	36 ± 1.27***	38 ± 0.44**	43 ± 1.76***	47 ± 1.08**	—
16	31 ± 1.45**	34 ± 1.35*	37 ± 1.22**	40 ± 1.89*	−7.83864
17	30 ± 1.82*	33 ± 1.37**	36 ± 1.55*	39 ± 0.68*	−4.93843
18	38 ± 1.03*	40 ± 0.64**	44 ± 1.78*	49 ± 1.16*	—
19	32 ± 0.23*	37 ± 1.44*	42 ± 0.46**	45 ± 0.82*	—
20	30 ± 1.63*	34 ± 1.02**	39 ± 0.16*	41 ± 1.92*	−8.67037
21	35 ± 1.53*	38 ± 1.47*	42 ± 0.26*	46 ± 1.36**	−9.32301
22	39 ± 1.23*	41 ± 0.64***	49 ± 0.18**	54 ± 1.83*	—
23	37 ± 1.75*	38 ± 1.35*	41 ± 1.47**	43 ± 1.54*	—
24	31 ± 1.27*	34 ± 1.72*	36 ± 0.28**	39 ± 1.14**	−9.4872
Indomethacin	41 ± 0.48*	58 ± 1.26**	49 ± 0.28*	13 ± 0.24*	—

Significance levels **p* < 0.05, ***p* < 0.01 and ****p* < 0.001 as compared with the respective control.

All the results were expressed as means ± SEM (standard error of estimate).

Table 3

Ulcerogenic activity of the most active 2,3-diaryl-3H-quinazolin-4-ones and indomethacin in rats

Compound	Dose (mg/kg)	Ulcer Lesion index (cm)
18	100	0
19	100	0
Indomethacin	10	1.42 ± 0.32
	50	11.48 ± 0.6

algorithm could not insert six compounds (**11**, **15**, **18**, **19**, **22** and **23**) into the active site of COX-2 enzyme owing to spatial constraints. It may also be observed that the studied compounds are bulkier than crystal bound ligand SC-558. The active site of the enzyme has opened up enough to accommodate a smaller molecule like SC-558 could not accommodate diaryl bicyclic compounds with halogen atoms of larger van der Waal's radii. Only four compounds **17**, **20**, **21** and **24** among docked compounds adopt a disposition exactly matching that of SC558 (Figs. 3 and 4). In particular, the unsubstituted/substituted phenyl moiety is inserted inside the COX-2 hydrophobic pocket while the methyl sulfonyl group is positioned into the selectivity pocket as the corresponding moiety

of SC558. It can be observed from the Figures 3 and 4 that the docked ligand does not form hydrogen bonding interactions with either Arg 120, Tyr 355 or His 90. The high scoring ligands (compounds **20**, **21** and **24**) are the ones with either fluoro substitution in 7th position of quinazolinone ring or 4 methoxy phenyl substitution of 2nd position of the quinazolinone ring. However, compound **17**, which adopts a favorable disposition as that of the SC-558 is among the low scoring ligands for no conceivable reasons. Compound **16** which is non-sulfonyl methyl top scoring ligand adopts favorable disposition as that of the SC-558 by aligning its thiomethyl group with sulphonamide group of the SC-558 (Figs. 5 and 6). The rest of the compounds does not adopts a favorable disposition as that of SC-558 is a resultant of dubious docking brought about by spatial constraints in the active site. Comparison of the enzyme inhibitory potency data with glide score suggest that docking results concurs with the biological evaluation results moderately in case of compounds with methyl sulfonyl groups since only one compound **17** is predicted poorly. In case of non sulfonyl methyl compounds, no meaningful conclusion could be made owing to availability of only two data points. Though the docking results were proven to be reasonably fair, it must also be noted that the compounds **18** and **19** were left out by the program were the most potent inhibitors of COX-2 in the series. The greater potency of these compounds indicates a greater flexibility of the COX-2 enzyme.

3. Conclusion

In conclusion, we describe herein the analogue-based design of a series 2,3-diaryl quinazolinones possessing methyl sulfanyl/methyl sulfonyl pharmacophore for in vitro and in vivo biological evaluation as COX-2 inhibitors. All the methyl sulfonyl substituted quinazolinones exhibited promising anti-inflammatory activity. In particular, 6-bromo-3-(4-methanesulfonyl-phenyl)-2-phenyl-3H-quinazolin-4-one (**18**), 7-chloro-3-(4-methanesulfonyl-phenyl)-2-phenyl-3H-quinazolin-4-one (**19**), 3-(4-methanesulfonyl-phenyl)-2-(4-methoxy-phenyl)-3H-quinazolin-4-one (**21**) and 6-bromo-3-(4-methanesulfonyl-phenyl)-2-(4-methoxy-phenyl)-3H-quinazolin-4-one (**22**) emerged as the most active compounds in the series. The results of ulcerogenic activity assay suggest that these compounds are gastric safe compared to indomethacin. The GLIDE based molecular docking results are reasonably fair in understanding the binding interactions and in vitro anti-inflammatory

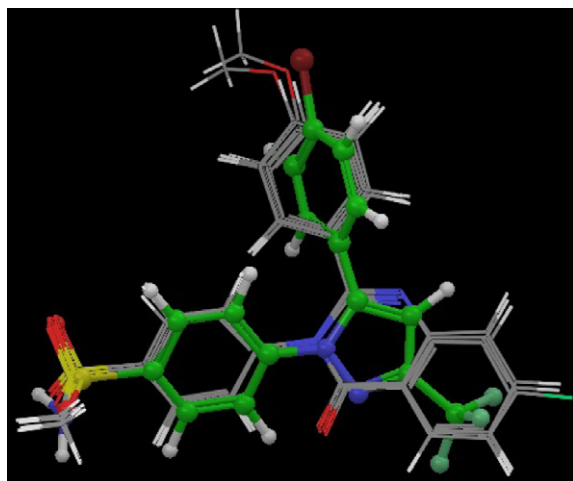


Figure 3. Alignment of docking poses of compounds **17**, **20**, **21** and **24** of 2,3-diaryl-3H-quinazolin-4-ones with SC-558.

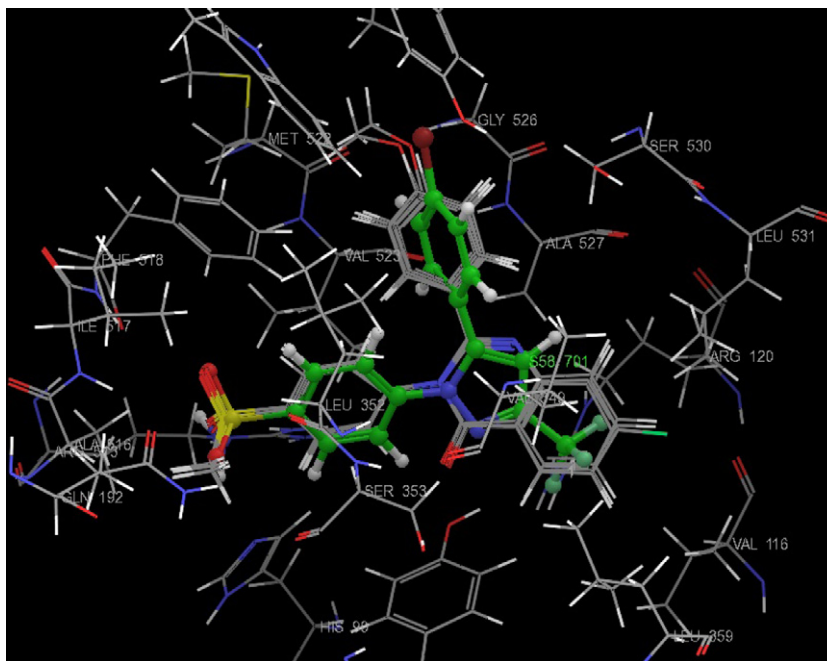


Figure 4. Alignment of docking poses of compounds **17**, **20**, **21** and **24** of 2,3-diaryl-3H-quinazolin-4-ones with SC-558 in active site of COX-2 enzyme.

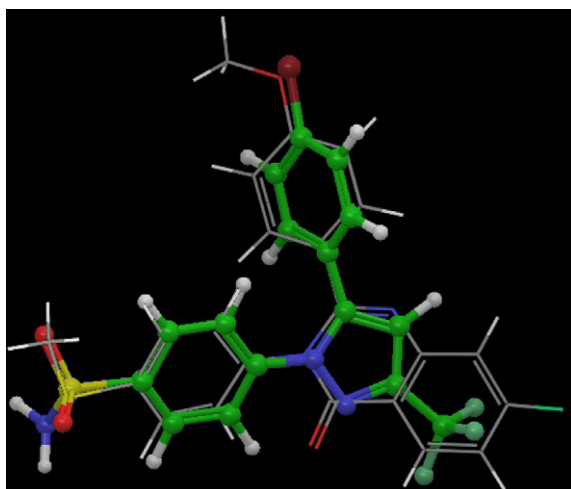


Figure 5. Alignment of docking pose of compound **16** of 2,3-diaryl-3H-quinazolin-4-ones with SC-558.

activity of these compounds to COX-2 enzyme. The present investigation suggests that 2,3-diaryl quinazolinones as a promising template for the design of new gastric safe anti-inflammatory agents, which can be further explored for anti-inflammatory activity. Further studies and related analogs will be reported in due course.

4. Experimental

4.1. Materials

All commercially available solvents and reagents were used without further purification. The starting materials were procured from Merck and Sigma Aldrich or prepared using known procedures. Column chromatographic separations were carried out by gradient elution with hexane-ethyl acetate mixture, unless otherwise mentioned and silica gel (60–120 mesh) used. TLC was performed on E-Merck pre-coated 60 F₂₅₄ plates and the spots were

rendered visible by exposing to UV light and iodine vapor. Melting points were recorded using an electrothermal melting point apparatus and are uncorrected. IR spectra were recorded using Shimadzu FTIR or Jasco FT/IR-470 PLUS. NMR spectral study was carried out using Bruker DRX 400. The FAB mass spectra were recorded on JEOL SX 102/DA-6000. Microanalytical data were obtained using a Carlo-Erba CHNS-O EA 1108 Elemental Analyser. Elemental analyses observed for all the newly synthesized compounds were within the limits of accuracy ($\pm 0.3\%$). Topological polar surface area (TPSA) and molecular volume were calculated using the web-based program Molinspiration.

4.2. Synthesis

4.2.1. Synthesis of substituted 2,3-diaryl-3H-quinazolin-4-ones (9–16)

Equimolar amount of substituted 2-phenyl-3H-benzoxazin-4-ones (0.02 mol) and 4-thiomethyl aniline (0.02 mol) in glacial acetic acid was refluxed for 2–4 h. A catalytic amount of PTSA was added to the reaction mixture. After completion of the reaction, the reaction mixture was cooled to room temperature and poured into crushed ice. The product formed was filtered; vacuum dried and crystallized using absolute ethanol.

4.2.1.1. 3-(4-Methylsulfanyl-phenyl)-2-phenyl-3H-quinazolin-4-one (9). Yield, 75%; mp 226–228 °C; R_f = 0.54 mobile phase toluene-ethyl acetate (7:3); IR (KBr, cm^{-1}): 1684 (C=O stretch); 1620 (C=N stretch); ^1H NMR (DMSO): δ 2.47 (s, 3H, S-CH₃), 7.27–7.32 (m, 3H), 7.54–7.69 (m, 6H), 7.90–7.93 (m, 3H), 8.47 (br d, J = 8.1 Hz, 1H); FAB-MS m/z [M+H]⁺: 345; Elemental Anal. Calcd for C₂₁H₁₆N₂OS: C, 73.23; H, 4.68; N, 8.13. Found: C, 73.26; H, 4.65; N, 8.15.

4.2.1.2. 6-Bromo-3-(4-methylsulfanyl-phenyl)-2-phenyl-3H-quinazolin-4-one (10). Yield: 72%, mp 219–220 °C; R_f = 0.48 mobile phase toluene-ethyl acetate (7:3); IR (KBr, cm^{-1}): 1672 (C=O stretch); 1622 (C=N stretch); ^1H NMR (DMSO): δ 2.49 (s, 3H, S-CH₃), 7.28–7.31 (d, 2H), 7.54–7.67 (m, 5H), 7.77–7.82 (dd, 1H), 7.89–7.91 (d, 2H), 8.09 (s, 1H), 8.42 (br d, J = 8.1 Hz, 1H); FAB-MS

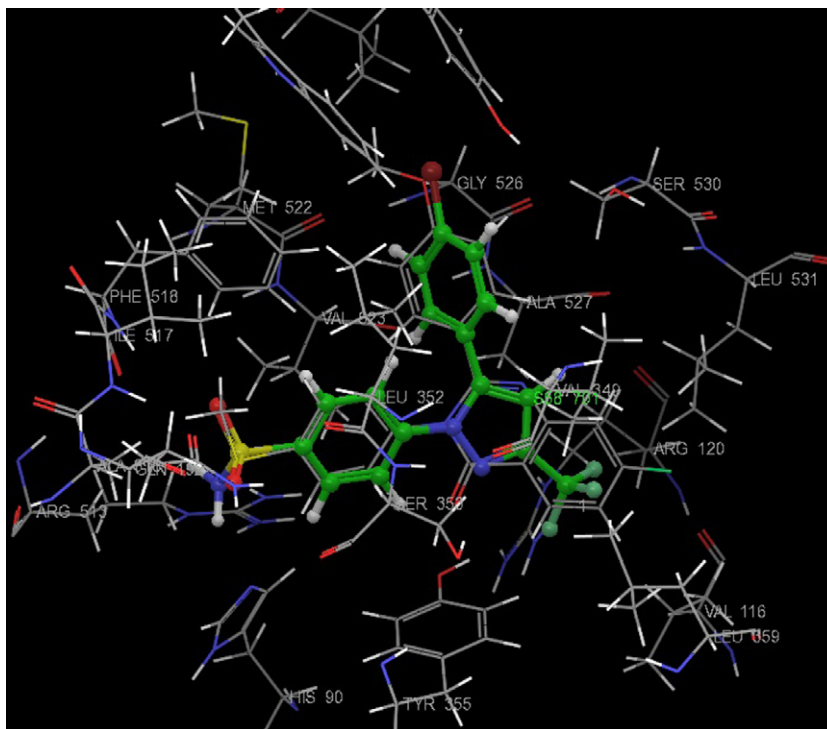


Figure 6. Alignment of docking poses of compound **16** of 2,3-diaryl-3H-quinazolin-4-ones with SC-558 in active site of COX-2 enzyme.

m/z $[M+H]^+$: 423; Elemental Anal. Calcd for $C_{21}H_{15}BrN_2OS$: C, 59.58; H, 3.57; N, 6.62. Found: C, 59.60; H, 3.56; N, 6.65.

4.2.1.3. 7-Chloro-3-(4-methylsulfanyl-phenyl)-2-phenyl-3H-quinazolin-4-one (11). Yield: 81%; mp 234–236 °C; R_f = 0.44 mobile phase toluene–ethyl acetate (7:3); IR (KBr, cm^{-1}): 1680 (C=O stretch); 1620 (C=N stretch); 1H NMR (DMSO): δ 2.49 (s, 3H, S-CH₃), 7.28–7.32 (m, 3H), 7.55–7.67 (m, 5H), 7.90–7.93 (m, 3H), 8.63 (br d, J = 8.1 Hz, 1H); FAB-MS m/z $[M+H]^+$: 380; Elemental Anal. Calcd for $C_{21}H_{15}ClN_2OS$: C, 66.57; H, 3.99; N, 7.39. Found: C, 66.55; H, 3.98; N, 7.41.

4.2.1.4. 7-Fluoro-3-(4-methylsulfanyl-phenyl)-2-phenyl-3H-quinazolin-4-one (12). Yield: 70%; mp 238–240 °C; R_f = 0.42 mobile phase toluene–ethyl acetate (7:3); IR (KBr, cm^{-1}): 1682 (C=O stretch); 1622 (C=N stretch); 1H NMR (DMSO): δ 2.47 (s, 3H, S-CH₃), 7.13–7.19 (m, 3H), 7.56–7.67 (m, 5H), 7.91–8.08 (m, 3H), 8.46 (br d, J = 8.1 Hz, 1H); FAB-MS m/z $[M+H]^+$: 363; Elemental Anal. Calcd for $C_{21}H_{15}FN_2OS$: C, 69.59; H, 4.17; N, 7.73. Found: C, 69.63; H, 4.21; N, 7.76.

4.2.1.5. 2-(4-Methoxy-phenyl)-3-(4-methylsulfanyl-phenyl)-3H-quinazolin-4-one (13). Yield: 65%; mp 122–124 °C; R_f = 0.40 mobile phase toluene–ethyl acetate (7:3); IR (KBr, cm^{-1}): 1677 (C=O stretch); 1620 (C=N stretch); 1H NMR (DMSO): δ 2.48 (s, 3H, S-CH₃), 3.78 (s, 3H, -OCH₃), 7.06–7.43 (m, 8H), 7.50–7.54 (m, 1H), 7.81–7.83 (m, 2H), 8.46 (br d, J = 8.1 Hz, 1H); FAB-MS m/z $[M+H]^+$: 375; Elemental Anal. Calcd for $C_{22}H_{18}N_2O_2S$: C, 70.57; H, 4.85; N, 7.48. Found: C, 70.61; H, 4.88; N, 7.51.

4.2.1.6. 6-Bromo-2-(4-methoxy-phenyl)-3-(4-methylsulfanyl-phenyl)-3H-quinazolin-4-one (14). Yield: 68%; mp 122–124 °C; R_f = 0.41 mobile phase toluene–ethyl acetate (7:3); IR (KBr, cm^{-1}): 1668 (C=O stretch); 1620 (C=N stretch); 1H NMR (DMSO): δ 2.50 (s, 3H, S-CH₃), 3.74 (s, 3H, -OCH₃), 7.08–7.46 (m, 7H), 7.52–

7.54 (m, 1H), 7.82–7.83 (m, 2H), 8.48 (br d, J = 8.1 Hz, 1H); FAB-MS m/z $[M+H]^+$: 453; Elemental Anal. Calcd for $C_{22}H_{17}BrN_2O_2S$: C, 58.28; H, 3.78; N, 6.18. Found: C, 58.27; H, 3.81; N, 6.20.

4.2.1.7. 7-Chloro-2-(4-methoxy-phenyl)-3-(4-methylsulfanyl-phenyl)-3H-quinazolin-4-one (15). Yield: 72%; mp 122–124 °C; R_f = 0.44 mobile phase toluene–ethyl acetate (7:3); IR (KBr, cm^{-1}): 1670 (C=O stretch); 1618 (C=N stretch); 1H NMR (DMSO): δ 2.51 (s, 3H, S-CH₃), 3.69 (s, 3H, -OCH₃), 7.04–7.42 (m, 7H), 7.50–7.53 (m, 1H), 7.82–7.83 (m, 2H), 8.39 (br d, J = 8.1 Hz, 1H); FAB-MS m/z $[M+H]^+$: 409; Elemental Anal. Calcd for $C_{22}H_{17}ClN_2O_2S$: C, 64.62; H, 4.19; N, 6.85. Found: C, 64.64; H, 4.22; N, 6.89.

4.2.1.8. 7-Fluoro-2-(4-methoxy-phenyl)-3-(4-methylsulfanyl-phenyl)-3H-quinazolin-4-one (16). Yield: 69%; mp 122–124 °C; R_f = 0.39 mobile phase toluene–ethyl acetate (7:3); IR (KBr, cm^{-1}): 1672 (C=O stretch); 1622 (C=N stretch); 1H NMR (DMSO): δ 2.49 (s, 3H, S-CH₃), 3.76 (s, 3H, -OCH₃), 7.10–7.42 (m, 7H), 7.48–7.52 (m, 1H), 7.81–7.84 (m, 2H), 8.41 (br d, J = 8.1 Hz, 1H); FAB-MS m/z $[M+H]^+$: 393; Elemental Anal. Calcd for $C_{22}H_{17}FN_2O_2S$: C, 67.33; H, 4.37; N, 7.14. Found: C, 67.35; H, 4.35; N, 7.15.

4.2.2. Oxidation of 4-methylsulfanyl substituted 2,3-diaryl-3H-quinazolin-4-ones (17–24)

A solution of oxone in H₂O (6 ml) and methanol (4 ml) was added dropwise to a solution of 4-methyl sulfanyl compounds (0.015 mol) in THF (10 ml) at 25 °C with stirring. The reaction was allowed to proceed for 2–3 h prior to addition of H₂O (10 ml) and extraction with CH₂Cl₂ (4 × 30 ml). The organic layer was separated and dried over anhydrous Na₂SO₄. The solvent was removed in vacuo, and the residue was purified by silica gel column chromatography.

4.2.2.1. 3-(4-Methanesulfonyl-phenyl)-2-phenyl-3H-quinazolin-4-one (17). Yield: 61%, mp 256–258 °C; R_f = 0.51 mobile phase toluene–ethyl acetate (7:3); IR (KBr, cm^{-1}): 1722 (C=O stretch);

1624 (C=N stretch); ^1H NMR (DMSO): δ 3.34 (s, 3H, SO_2CH_3), 7.15–7.41 (m, 2H), 7.53–7.68 (m, 5H), 7.82–7.86 (m, 1H), 7.90–7.96 (m, 3H), 8.32 (br d, $J = 8.1$ Hz, 1H); FAB-MS m/z $[\text{M}+\text{H}]^+$: 377; Elemental Anal. Calcd for $\text{C}_{21}\text{H}_{16}\text{N}_2\text{O}_3\text{S}$: C, 67.00; H, 4.28; N, 7.44. Found: C, 67.02; H, 4.30; N, 7.47.

4.2.2.2. 6-Bromo-3-(4-methanesulfonyl-phenyl)-2-phenyl-3H-quinazolin-4-one (18). Yield: 54%; mp 248–251 °C; $R_f = 0.49$ mobile phase toluene–ethyl acetate (7:3); IR (KBr, cm^{-1}): 1688 (C=O stretch); 1625 (C=N stretch); ^1H NMR (DMSO): δ 3.31 (s, 3H, SO_2CH_3), 7.16–7.41 (m, 2H), 7.54–7.68 (m, 4H), 7.82–7.86 (m, 1H), 7.91–7.96 (m, 3H), 8.34 (br d, $J = 8.1$ Hz, 1H); FAB-MS m/z $[\text{M}+\text{H}]^+$: 455; Elemental Anal. Calcd for $\text{C}_{21}\text{H}_{15}\text{BrN}_2\text{O}_3\text{S}$: C, 55.39; H, 3.32; N, 6.15. Found: C, 55.42; H, 3.33; N, 6.17.

4.2.2.3. 7-Chloro-3-(4-methanesulfonyl-phenyl)-2-phenyl-3H-quinazolin-4-one (19). Yield: 75%; mp 230–232 °C; $R_f = 0.54$ mobile phase toluene–ethyl acetate (7:3); IR (KBr, cm^{-1}): 1672 (C=O stretch); 1620 (C=N stretch); ^1H NMR (DMSO): δ 3.32 (s, 3H, SO_2CH_3), 7.18–7.42 (m, 2H), 7.56–7.68 (m, 4H), 7.82–7.86 (m, 1H), 7.92–7.98 (m, 3H), 8.34 (br d, $J = 8.1$ Hz, 1H); FAB-MS m/z $[\text{M}]^+$: 410; Elemental Anal. Calcd for $\text{C}_{21}\text{H}_{15}\text{ClN}_2\text{O}_3\text{S}$: C, 61.39; H, 3.68; N, 6.82. Found: C, 61.41; H, 3.71; N, 6.86.

4.2.2.4. 7-Fluoro-3-(4-methanesulfonyl-phenyl)-2-phenyl-3H-quinazolin-4-one (20). Yield: 66%; mp 262–264 °C; $R_f = 0.47$ mobile phase toluene–ethyl acetate (7:3); IR (KBr, cm^{-1}): 1672 (C=O stretch); 1618 (C=N stretch); ^1H NMR (DMSO): δ 3.32 (s, 3H, SO_2CH_3), 7.12–7.39 (m, 2H), 7.53–7.64 (m, 4H), 7.82–7.86 (m, 1H), 7.90–7.94 (m, 3H), 8.34 (br d, $J = 8.1$ Hz, 1H); FAB-MS m/z $[\text{M}+\text{H}]^+$: 395; Elemental Anal. Calcd for $\text{C}_{21}\text{H}_{15}\text{FN}_2\text{O}_3\text{S}$: C, 63.95; H, 3.83; N, 7.10. Found: C, 63.96; H, 3.84; N, 7.12.

4.2.2.5. 3-(4-Methanesulfonyl-phenyl)-2-(4-methoxy-phenyl)-3H-quinazolin-4-one (21). Yield: 68%; mp 234–235 °C; $R_f = 0.42$ mobile phase toluene–ethyl acetate (7:3); IR (KBr, cm^{-1}): 1676 (C=O stretch); 1620 (C=N stretch); ^1H NMR (DMSO): δ 3.26 (s, 3H, SO_2CH_3), 3.60 (s, 3H, $-\text{OCH}_3$), 7.14–7.48 (m, 8H), 7.56–7.60 (m, 1H), 7.82–7.84 (m, 2H), 8.51 (br d, $J = 8.1$ Hz, 1H); FAB-MS m/z $[\text{M}+\text{H}]^+$: 408; Elemental Anal. Calcd for $\text{C}_{22}\text{H}_{18}\text{N}_2\text{O}_4\text{S}$: C, 65.01; H, 4.46; N, 6.89. Found: C, 65.03; H, 4.46; N, 6.88.

4.2.2.6. 6-Bromo-3-(4-methanesulfonyl-phenyl)-2-(4-methoxy-phenyl)-3H-quinazolin-4-one (22). Yield: 60%; mp 253–255 °C; $R_f = 0.40$ mobile phase toluene–ethyl acetate (7:3); IR (KBr, cm^{-1}): 1672 (C=O stretch); 1624 (C=N stretch); ^1H NMR (DMSO): δ 3.24 (s, 3H, SO_2CH_3), 3.71 (s, 3H, $-\text{OCH}_3$), 7.18–7.52 (m, 7H), 7.55–7.61 (m, 1H), 7.82–7.84 (m, 2H), 8.52 (br d, $J = 8.1$ Hz, 1H); FAB-MS m/z $[\text{M}+\text{H}]^+$: 485; Elemental Anal. Calcd for $\text{C}_{22}\text{H}_{17}\text{BrN}_2\text{O}_4\text{S}$: C, 54.44; H, 3.53; N, 5.77. Found: C, 54.46; H, 3.55; N, 5.78.

4.2.2.7. 7-Chloro-3-(4-methanesulfonyl-phenyl)-2-(4-methoxy-phenyl)-3H-quinazolin-4-one (23). Yield: 70%; mp: 217–218 °C; $R_f = 0.42$ mobile phase toluene–ethyl acetate (7:3); IR (KBr, cm^{-1}): 1680 (C=O stretch); 1622 (C=N stretch); ^1H NMR (DMSO): δ 3.20 (s, 3H, SO_2CH_3), 3.72 (s, 3H, $-\text{OCH}_3$), 7.18–7.52 (m, 7H), 7.55–7.61 (m, 1H), 7.84–7.86 (m, 2H), 8.51 (br d, $J = 8.1$ Hz, 1H); FAB-MS m/z $[\text{M}+\text{H}]^+$: 441; Elemental Anal. Calcd for $\text{C}_{22}\text{H}_{17}\text{ClN}_2\text{O}_4\text{S}$: C, 59.93; H, 3.89; N, 6.35. Found: C, 59.96; H, 3.87; N, 6.34.

4.2.2.8. 7-Fluoro-3-(4-methanesulfonyl-phenyl)-2-(4-methoxy-phenyl)-3H-quinazolin-4-one (24). Yield: 62%; mp 248–250 °C; $R_f = 0.41$ mobile phase toluene–ethyl acetate (7:3); IR (KBr, cm^{-1}): 1686 (C=O stretch); 1620 (C=N stretch); ^1H NMR (DMSO): δ 3.18 (s, 3H, SO_2CH_3), 3.69 (s, 3H, $-\text{OCH}_3$), 7.09–7.49 (m, 7H), 7.54–7.60 (m, 1H), 7.84–7.86 (m, 2H), 8.52 (br d, $J = 8.1$ Hz, 1H); FAB-MS

m/z $[\text{M}+\text{H}]^+$: 425; Elemental Anal. Calcd for $\text{C}_{22}\text{H}_{17}\text{FN}_2\text{O}_4\text{S}$: C, 62.25; H, 4.04; N, 6.60. Found: C, 62.26; H, 4.07; N, 6.61.

4.3. Biological evaluation

4.3.1. In vitro COX-1 and COX-2 inhibitory assay

The in vitro ability of substituted 2,3-diaryl-3H-quinazolin-4-ones and celecoxib to inhibit the COX-1 and COX-2 isozymes was carried out using cayman colorimetric COX (ovine) inhibitor screening assay kit (Catalog No. 760111) supplied by Cayman chemicals, USA. The calculations were performed as per the kit guidelines.³⁸

4.3.2. Animals

Animals were assigned into several groups randomly and each group consists of six animals. The animals were kept in appropriate cages at temperature controlled (25 ± 2 °C) rooms, under a 12 h light and dark cycle and they were fed standard rodent pellet. All the animals were acclimatized for a week before the experiment. Standard ethical guidelines of Committee for the Purpose of Control and Supervision of Experiments on Animals (CPCSEA), Ministry of Social Justice and Empowerment, Government of India were followed.

4.3.3. Dose preparation

The test compounds and the standard drugs were administered orally in the form of a suspension in 1% or 0.5% carboxy methylcellulose sodium (CMC-Na).

4.3.4. In vivo anti-inflammatory activity carrageenan-induced rat paw edema assay method

Anti-inflammatory activity was determined using carrageenan-induced foot paw edema assay method in rats using indomethacin 10 mg/kg as standard drug.³⁹ The test compounds were administered orally at a dose of 50 mg/kg. Edemas were produced by injecting 0.1 ml of a solution of carrageenan in the hind paw. Paw volumes were measured using the mercury displacement technique with the help of a plethysmograph immediately before and 90, 180, 270 and 360 min after carrageenan injection. The percentage of edema inhibition was calculated using the following formula.

$$\text{Percentage of edema inhibition} = 100[1 - (A - X)/(B - Y)]$$

Where, X is the mean paw volume of rats before the administration of carrageenan and test compounds or reference drugs; A and B is the mean paw volume of rats after the administration of carrageenan in the test group and control group, respectively; Y is the mean paw volume of rats before the administration of carrageenan in the control group.

4.3.5. Ulcerogenic activity

Albino rats of Wister strain weighing 150–200 g of either sex were distributed at random in groups of 10 animals each. Test compounds were administered by oral route at a dose of 100 mg/kg once daily for four consecutive days. The other group of animals was administered with vehicle alone (control) and or indomethacin (reference) at dose of 10, 50 mg/kg for inter-assay comparison. The animals were killed under deep ether anesthesia and stomachs were removed. Then the abdomen of each rat was opened through great curvature and examined under dissecting microscope for lesions or bleedings. In macroscopic examination, the severity of the mucosal damage (ulcerogenic index) was graduated by means of scores.⁴⁰

In microscopic evaluation, the tissue pieces were placed in 10% buffered formaldehyde solution for one week in room temperature to fix the tissue. After washing, the tissues were dehydrated in

ascending degrees of ethanol, cleared in xylene and embedded in paraffin pastilles serial sections of 5 μm were cut and stained with hematoxylin-eosin. Sections that showed effects of compounds and reference drugs were selected, examined and photographed by using light microscope.

4.3.6. Acute toxicity study

After completion of all experiments, the animals were observed for 3 days for signs of toxicity, mortality and behavioral changes.

4.3.7. Statistical analysis

Statistical significance of anti-inflammatory activity of the compounds on rat paw edema model was analyzed using one-way analysis of variance (ANOVA) followed by Dunnett's multiple comparison test. A significance level of $P < 0.05$ was considered as acceptable in all cases. All the results were expressed as mean \pm SEM (standard error of estimate).

4.4. Molecular docking

Docking studies of synthesized compounds listed in Table 2 were performed using crystal structure of COX-2 enzyme (PDB ID: 1CX2) obtained from the RCSB Protein Data Bank, which houses the selective COX-2 inhibitor SC-558 in its active site.⁴¹ The structure of the chain 'A' was chosen as the target for docking studies. All the experiments were performed using the program GLIDE (Grid-based Ligand Docking with Energetics) module version 4.5, Schrödinger, LLC, New York, NY, 2007 (Schrodinger Inc.). Coordinates of the full-length substrate-complexed tetramer were prepared for Glide 4.0 calculations by running the protein preparation wizard. The *p*-prep script produces a new receptor file in which all residues are neutralized except those that are relatively close to the ligand (if the protein is complexed with a ligand) or form salt bridges. The *impref* script runs a series of restrained impact energy minimizations using the Impact utility. Minimizations were run until the average root mean square deviation (rmsd) of the non-hydrogen atoms reached 0.3 Å°.

Glide uses two boxes that share a common centre to organize its calculations: a larger enclosing box and a smaller binding box. The grids themselves are calculated within the space defined by the enclosing box. The binding box defines the space through which the centre of the defined ligand will be allowed to move during docking calculations. It provides a measure of the effective size of the search space. The only requirement on the enclosing box is that it be large enough to contain all ligand atoms, even when the ligand centre is placed at an edge or vertex of the binding box. Grid files were generated using the cocrystallized ligand at the centre of the two boxes. The size of the binding box was set at 20 Å° in order to explore a large region of the protein. The three-dimensional structures of the compounds were constructed using the Maestro interface. The initial geometry of the structures was optimized using the OPLS-2005 force field performing 1000 steps of conjugate gradient minimization. The compounds were subjected to flexible docking using the pre-computed grid files. For each compound the 100 top-scored poses were saved and analyzed and only the best scoring poses were selected for the study.

Acknowledgments

Author E.M. thankful to University Grants Commission and All India Council for Technical Education, New Delhi, Govt. of India

for financial support in the form of JRF and Career Award for Young Teachers (CAYT) Scheme.

References and notes

- Botting, J. H. *Drugs Today* **1999**, 35, 225.
- Vane, J. R. *Nat. New Biol.* **1971**, 231, 232.
- Vane, J. R.; Bakhle, Y. S.; Botting, R. M. *Annu. Rev. Pharmacol. Toxicol.* **1998**, 38, 97.
- Raz, A.; Wyche, A.; Siegel, N.; Needleman, P. J. *Biol. Chem.* **1988**, 263, 3022.
- Fu, J. Y.; Masferrer, J. L.; Siebert, K.; Raz, A.; Needleman, P. J. *Biol. Chem.* **1990**, 265, 16737.
- Kurumbail, R. G.; Stevens, A. M.; Gierse, J. K.; McDonald, J. J.; Stegeman, R. A.; Pak, J. Y.; Gildehaus, D.; Miyashiro, J. M.; Penning, T. D.; Seibert, K.; Isakson, P. C.; Stallings, W. C. *Nature* **1996**, 384, 644.
- Kalgutkar, A. S.; Zhao, Z. *Curr. Drug Targets* **2001**, 2, 79.
- Moore, B. C.; Simmons, D. L. *Curr. Med. Chem.* **2000**, 7, 1131.
- Song, X.; Lin, H. P.; Johnson, A. J.; Tseng, P. H.; Yang, Y. T. *J. Natl. Cancer Inst.* **2002**, 94, 585.
- Smythies, J. *Proc. R. Soc. London, Ser. B* **1996**, 263, 487.
- McGeer, P. L.; McGeer, E. G. *J. Leukocyte Biol.* **1999**, 65, 409.
- Dannhardt, G.; Kiefer, W. *Eur. J. Med. Chem.* **2000**, 36, 109.
- Penning, T. D.; Talley, J. J.; Bertenshaw, S. R.; Carter, J. S.; Collins, P. W.; Doctor, S.; Graneto, M. J.; Lee, L. F.; Malecha, J. W.; Miyashiro, J. M.; Rogers, R. S.; Rogier, D. J.; Yu, S. S.; Anderson, G. D.; Burton, E. G.; Cogburn, J. N.; Gregory, S. A.; Koboldt, C. M.; Perkins, W. E.; Seibert, K.; Veenhuizen, A. W.; Zhang, Y. Y.; Isakson, P. C. *J. Med. Chem.* **1997**, 40, 1347.
- Bertenshaw, S. R.; Talley, J. J.; Rogier, D. J.; Graneto, M. J.; Koboldt, C. M.; Zhang, Y. *Bioorg. Med. Chem. Lett.* **1996**, 6, 2827.
- Talley, J. J.; Bertenshaw, S. R.; Brown, D. L.; Carter, J. S.; Graneto, M. J.; Kellogg, M. S.; Koboldt, C. M.; Yuan, J.; Zhang, Y. Y.; Seibert, K. *J. Med. Chem.* **2000**, 43, 1661.
- Talley, J. J.; Brown, D. L.; Carter, J. S.; Graneto, M. J.; Koboldt, C. M.; Masferrer, J. L.; Perkins, W. E.; Rogers, R. S.; Shaffer, A. F.; Zhang, Y. Y.; Zweifel, B. S.; Seibert, K. *J. Med. Chem.* **2000**, 43, 775.
- Garg, R.; Kurup, A.; Mekapati, S. B.; Hansch, C. *Chem. Rev.* **2003**, 103, 703.
- Manivannan, E.; Chaturvedi, S. C. *Med. Chem.* **2009**, 5, 440.
- Manivannan, E.; Chaturvedi, S. C. *Med. Chem. Res.* **2009**, 18, 396.
- Prasanna, S.; Manivannan, E.; Chaturvedi, S. C. *J. Enzyme Inhib. Med. Chem.* **2005**, 20, 455.
- Prasanna, S.; Manivannan, E.; Chaturvedi, S. C. *Bioorg. Med. Chem. Lett.* **2005**, 15, 2097.
- Prasanna, S.; Manivannan, E.; Chaturvedi, S. C. *Bioorg. Med. Chem. Lett.* **2005**, 15, 313.
- Prasanna, S.; Manivannan, E.; Chaturvedi, S. C. *Arch. Pharm. (Weinheim)* **2004**, 337, 440.
- Prasanna, S.; Manivannan, E.; Chaturvedi, S. C. *Bioorg. Med. Chem. Lett.* **2004**, 14, 4005.
- Prasanna, S.; Manivannan, E.; Chaturvedi, S. C. *QSAR Comb. Sci.* **2004**, 23, 621.
- Manivannan, E.; Prasanna, S.; Chaturvedi, S. C. *Indian J. Biochem. Biophys.* **2004**, 41, 179.
- Jawabrah, B.; Hourani, A.; Sharma, S. K.; Mane, J. Y.; Tuszyński, J.; Baracos, V.; Kniess, T.; Suresh, M.; Pietzsch, J.; Wuest, F. *Bioorg. Med. Chem. Lett.* **2011**, 21, 1823.
- Singh, S. K.; Saibaba, V.; Ravikumar, V.; Santosh, V.; Rudrawar, Daga, P.; Rao, C. S.; Akhila, V.; Hegde, P.; Rao, K. Y. *Bioorg. Med. Chem. Lett.* **2004**, 12, 1881.
- Uddin, Md. J.; Rao, P. N. P.; Knaus, E. E. *Bioorg. Med. Chem.* **2004**, 12, 5929.
- Singh, P.; Mittal, A.; Kaur, S.; Kumar, S. *Bioorg. Med. Chem.* **2006**, 14, 7910.
- Moon, T. C.; Murakami, M.; Kudo, I.; Son, K. H.; Kim, H. P.; Kang, S. S.; Chang, H. W. *Inflamm. Res.* **1999**, 48, 621.
- Chiou, W. F.; Liao, J. P.; Chen, C. F. *J. Nat. Prod.* **1996**, 59, 374.
- Lee, S. H.; Son, J. K.; Jeong, B. S.; Jeong, T. C.; Chang, H. W.; Lee, E. S.; Jahng, Y. D. *Molecule* **2008**, 13, 272.
- Danz, H.; Stoyanova, S.; Wippich, P.; Brattström, A.; Hamburger, M. *Planta Med.* **2001**, 67, 411.
- Wu, X. Y.; Qin, G. W.; Cheung, K. K.; Cheng, K. F. *Tetrahedron* **1997**, 53, 13323.
- Hartle, I.; Seifert, K. *Planta Med.* **1994**, 60, 578.
- Kumar, A.; Sharma, S.; Archana; Bajaj, K.; Sharma, S.; Panwar, H.; Singh, T.; Srivastava, V. K. *Bioorg. Med. Chem.* **2003**, 11, 5293.
- Lee, S. H.; Son, M. J.; Ju, H. K.; Lin, C. X.; Moon, T. C.; Choi, H. G.; Son, J. K.; Chang, H. W. *Biol. Pharm. Bull.* **2004**, 27, 786.
- Winter, C. A.; Risley, E. A.; Nuss, G. W. *Proc. Soc. Exp. Biol. Med.* **1962**, 111, 544.
- Milanino, R.; Concar, E.; Conforti, A.; Marrella, M.; Franco, L.; Moretti, U.; Velo, G.; Rainsford, K. D.; Bressan, M. *Eur. J. Med. Chem.* **1988**, 23, 217.
- Friesner, R. A.; Murphy, R. B.; Repasky, M. P.; Frye, L. L.; Greenwood, J. R.; Halgren, T. A.; Sanschagrin, P. C.; Mainz, D. T. *J. Med. Chem.* **2006**, 49, 6177.